Pulsed Gamma-rays from the millisecond pulsar J0030+0451 with the Fermi Large Area Telescope

A.A. Abdo, Markus Ackermann, W. B. Atwood, Magnus Axelsson, Luca Baldini, Jean Ballet, Guido Barbiellini, D. Bastieri, M. Battelino, B. M. Baughman, et al.

The Astrophysical Journal, 699:1171–1177, 2009 July 10 doi:10.1088/0004-637X/699/2/1171

PULSED GAMMA RAYS FROM THE MILLISECOND PULSAR J0030+0451 WITH THE *FERMI* LARGE AREA TELESCOPE

A. A. Abdo[1,47], M. Ackermann[2], W. B. Atwood[3], M. Axelsson[4,5], L. Baldini[6], J. Ballet[7], G. Barbiellini[8,9], D. Bastieri[10,11], M. Battelino[4,12], B. M. Baughman[13], K. Bechtol[2], R. Bellazzini[6], B. Berenji[2], E. D. Bloom[2], E. Bonamente[14,15], A. W. Borgland[2], J. Bregeon[6], A. Brez[6], M. Brigida[16,17], P. Bruel[18], T. H. Burnett[19], G. A. Caliandro[16,17], R. A. Cameron[2], P. A. Caraveo[20], J. M. Casandjian[7], C. Cecchi[14,15], E. Charles[2], A. Chekhtman[1,21], C. C. Cheung[22], J. Chiang[2], S. Ciprini[14,15], R. Claus[2], I. Cognard[23], J. Cohen-Tanugi[24], L. R. Cominsky[25], J. Conrad[4,12,26], S. Cutini[27], C. D. Dermer[1], A. de Angelis[28], F. de Palma[16,17], S. W. Digel[2], M. Dormody[3], E. do Couto e Silva[2], P. S. Drell[2], R. Dubois[2], D. Dumora[29,30], C. Farnier[24], C. Favuzzi[16,17], W. B. Focke[2], M. Frailis[28], Y. Fukazawa[31], S. Funk[2], P. Fusco[16,17], F. Gargano[17], D. Gasparrini[27], N. Gehrels[22,32], S. Germani[14,15], B. Giebels[18], N. Giglietto[16,17], F. Giordano[16,17], T. Glanzman[2], G. Godfrey[2], I. A. Grenier[7], M.-H. Grondin[29,30], J. E. Grove[1], L. Guillemot[29,30], S. Guiriec[24], Y. Hanabata[31], A. K. Harding[22], M. Hayashida[2], E. Hays[22], R. E. Hughes[13], G. Jóhannesson[2], A. S. Johnson[2], R. P. Johnson[3], T. J. Johnson[32,22], W. N. Johnson[1], T. Kamae[2], H. Katagiri[31], J. Kataoka[33], N. Kawai[33,34], M. Kerr[19], J. Knödlseder[35], M. L. Kocian[2], N. Komin[7,24], F. Kuehn[13], M. Kuss[6], J. Lande[2], L. Latronico[6], S.-H. Lee[2], M. Lemoine-Goumard[29,30], F. Longo[8,9], F. Loparco[16,17], B. Lott[29,30], M. N. Lovellette[1], P. Lubrano[14,15], G. M. Madejski[2], A. Makeev[1,21], M. Marelli[20], M. N. Mazziotta[17], W. McConville[22,32], J. E. McEnery[22], C. Meurer[4,26], P. F. Michelson[2], W. Mitthumsiri[2], T. Mizuno[31], A. A. Moiseev[36], C. Monte[16,17], M. E. Monzani[2], A. Morselli[37], I. V. Moskalenko[2], S. Murgia[2], P. L. Nolan[2], E. Nuss[24], T. Ohsugi[31], N. Omodei[6], E. Orlando[38], J. F. Ormes[39], B. Pancrazi[35], D. Paneque[2], J. H. Panetta[2], D. Parent[29,30], M. Pepe[14,15], M. Pesce-Rollins[6], F. Piron[24], T. A. Porter[3], S. Rainò[16,17], R. Rando[10,11], M. Razzano[6], A. Reimer[2], O. Reimer[2], T. Reposeur[29,30], S. Ritz[22,32], L. S. Rochester[2], A. Y. Rodriguez[40], R. W. Romani[2], F. Ryde[4,12], H. F.-W. Sadrozinski[3], D. Sanchez[18], A. Sander[13], P. M. Saz Parkinson[3], C. Sgrò[6], E. J. Siskind[41], D. A. Smith[29,30], P. D. Smith[13], G. Spandre[6], P. Spinelli[16,17], J.-L. Starck[7], M. S. Strickman[1], D. J. Suson[42], H. Tajima[2], H. Takahashi[31], T. Tanaka[2], J. B. Thayer[2], J. G. Thayer[2], G. Theureau[23], D. J. Thompson[22], L. Tibaldo[10,11], D. F. Torres[40,43], G. Tosti[14,15], A. Tramacere[2,44], Y. Uchiyama[2], T. L. Usher[2], A. Van Etten[2], N. Vilchez[35], V. Vitale[37,45], A. P. Waite[2], K. Watters[2], N. Webb[35], K. S. Wood[1], T. Ylinen[4,12,46], and M. Ziegler[3]

[1] Space Science Division, Naval Research Laboratory, Washington, DC 20375, USA
[2] W. W. Hansen Experimental Physics Laboratory, Kavli Institute for Particle Astrophysics and Cosmology, Department of Physics and SLAC National Laboratory, Stanford University, Stanford, CA 94305, USA
[3] Santa Cruz Institute for Particle Physics, Department of Physics and Department of Astronomy and Astrophysics, University of California at Santa Cruz, Santa Cruz, CA 95064, USA
[4] The Oskar Klein Centre for Cosmo Particle Physics, AlbaNova, SE-106 91 Stockholm, Sweden
[5] Department of Astronomy, Stockholm University, SE-106 91 Stockholm, Sweden
[6] Istituto Nazionale di Fisica Nucleare, Sezione di Pisa, I-56127 Pisa, Italy
[7] Laboratoire AIM, CEA-IRFU/CNRS/Université Paris Diderot, Service d'Astrophysique, CEA Saclay, 91191 Gif sur Yvette, France
[8] Istituto Nazionale di Fisica Nucleare, Sezione di Trieste, I-34127 Trieste, Italy
[9] Dipartimento di Fisica, Università di Trieste, I-34127 Trieste, Italy
[10] Istituto Nazionale di Fisica Nucleare, Sezione di Padova, I-35131 Padova, Italy
[11] Dipartimento di Fisica "G. Galilei," Università di Padova, I-35131 Padova, Italy
[12] Department of Physics, Royal Institute of Technology (KTH), AlbaNova, SE-106 91 Stockholm, Sweden
[13] Department of Physics, Center for Cosmology and Astro-Particle Physics, The Ohio State University, Columbus, OH 43210, USA
[14] Istituto Nazionale di Fisica Nucleare, Sezione di Perugia, I-06123 Perugia, Italy
[15] Dipartimento di Fisica, Università degli Studi di Perugia, I-06123 Perugia, Italy
[16] Dipartimento di Fisica "M. Merlin" dell'Università e del Politecnico di Bari, I-70126 Bari, Italy
[17] Istituto Nazionale di Fisica Nucleare, Sezione di Bari, 70126 Bari, Italy
[18] Laboratoire Leprince-Ringuet, École polytechnique, CNRS/IN2P3, Palaiseau, France
[19] Department of Physics, University of Washington, Seattle, WA 98195-1560, USA; kerrm@u.washington.edu.
[20] INAF-Istituto di Astrofisica Spaziale e Fisica Cosmica, I-20133 Milano, Italy
[21] George Mason University, Fairfax, VA 22030, USA
[22] NASA Goddard Space Flight Center, Greenbelt, MD 20771, USA; Tyrel. J.Johnson@nasa.gov
[23] Laboratoire de Physique et Chemie de l'Environnement, LPCE UMR 6115 CNRS, F-45071 Orléans Cedex 02, and Station de radioastronomie de Nançay, Observatoire de Paris, CNRS/INSU, F-18330 Nançay, France
[24] Laboratoire de Physique Théorique et Astroparticules, Université Montpellier 2, CNRS/IN2P3, Montpellier, France
[25] Department of Physics and Astronomy, Sonoma State University, Rohnert Park, CA 94928-3609, USA
[26] Department of Physics, Stockholm University, AlbaNova, SE-106 91 Stockholm, Sweden
[27] Agenzia Spaziale Italiana (ASI) Science Data Center, I-00044 Frascati (Roma), Italy
[28] Dipartimento di Fisica, Università di Udine and Istituto Nazionale di Fisica Nucleare, Sezione di Trieste, Gruppo Collegato di Udine, I-33100 Udine, Italy
[29] CNRS/IN2P3, Centre d'Études Nucléaires Bordeaux Gradignan, UMR 5797, Gradignan, 33175, France; guillemo@cenbg.in2p3.fr
[30] Université de Bordeaux, Centre d'Études Nucléaires Bordeaux Gradignan, UMR 5797, Gradignan, 33175, France
[31] Department of Physical Science and Hiroshima Astrophysical Science Center, Hiroshima University, Higashi-Hiroshima 739-8526, Japan
[32] University of Maryland, College Park, MD 20742, USA
[33] Department of Physics, Tokyo Institute of Technology, Meguro City, Tokyo 152-8551, Japan
[34] Cosmic Radiation Laboratory, Institute of Physical and Chemical Research (RIKEN), Wako, Saitama 351-0198, Japan
[35] Centre d'Étude Spatiale des Rayonnements, CNRS/UPS, BP 44346, F-30128 Toulouse Cedex 4, France
[36] Center for Research and Exploration in Space Science and Technology (CRESST), NASA Goddard Space Flight Center, Greenbelt, MD 20771, USA
[37] Istituto Nazionale di Fisica Nucleare, Sezione di Roma "Tor Vergata," I-00133 Roma, Italy

[38] Max-Planck Institut für extraterrestrische Physik, 85748 Garching, Germany
[39] Department of Physics and Astronomy, University of Denver, Denver, CO 80208, USA
[40] Institut de Ciencies de l'Espai (IEEC-CSIC), Campus UAB, 08193 Barcelona, Spain
[41] NYCB Real-Time Computing Inc., Lattingtown, NY 11560-1025, USA
[42] Department of Chemistry and Physics, Purdue University Calumet, Hammond, IN 46323-2094, USA
[43] Institució Catalana de Recerca i Estudis Avançats (ICREA), Barcelona, Spain
[44] Consorzio Interuniversitario per la Fisica Spaziale (CIFS), I-10133 Torino, Italy
[45] Dipartimento di Fisica, Università di Roma "Tor Vergata," I-00133 Roma, Italy
[46] School of Pure and Applied Natural Sciences, University of Kalmar, SE-391 82 Kalmar, Sweden
Received 2009 January 16; accepted 2009 April 29; published 2009 June 19

ABSTRACT

We report the discovery of gamma-ray pulsations from the nearby isolated millisecond pulsar (MSP) PSR J0030+0451 with the Large Area Telescope on the *Fermi* Gamma-ray Space Telescope (formerly GLAST). This discovery makes PSR J0030+0451 the second MSP to be detected in gamma rays after PSR J0218+4232, observed by the EGRET instrument on the Compton Gamma-Ray Observatory. The spin-down power $\dot{E} = 3.5 \times 10^{33}$ erg s^{-1} is an order of magnitude lower than the empirical lower bound of previously known gamma-ray pulsars. The emission profile is characterized by two narrow peaks, 0.07 ± 0.01 and 0.08 ± 0.02 wide, respectively, separated by 0.44 ± 0.02 in phase. The first gamma-ray peak falls 0.15 ± 0.01 after the main radio peak. The pulse shape is similar to that of the "normal" gamma-ray pulsars. An exponentially cutoff power-law fit of the emission spectrum leads to an integral photon flux above 100 MeV of $(6.76 \pm 1.05 \pm 1.35) \times 10^{-8}$ cm^{-2} s^{-1} with cutoff energy $(1.7 \pm 0.4 \pm 0.5)$ GeV. Based on its parallax distance of (300 ± 90) pc, we obtain a gamma-ray efficiency $L_\gamma/\dot{E} \simeq 15\%$ for the conversion of spin-down energy rate into gamma-ray radiation, assuming isotropic emission.

Key words: gamma rays: observations – pulsars: general – pulsars: individual (PSR J0030+0451)

1. INTRODUCTION

Two distinct pulsar populations are the "normal" and "millisecond" pulsars (MSPs), the latter being rapidly rotating neutron stars ($P \lesssim 30$ ms) with very small period increases ($\dot{P} \lesssim 10^{-17}$ s s^{-1}). MSPs represent roughly 10% of the pulsars listed in the ATNF online catalog (Manchester et al. 2005). In the classical framework of the magnetic braking model, MSPs are old stars with characteristic spin-down ages $\tau = P/(2\dot{P}) \simeq (0.1\text{–}10) \times 10^9$ yr, and characteristic surface dipole magnetic fields, $B_{\rm surf} \simeq 3.2 \times 10^{19}(P\dot{P})^{1/2} < 10^{10}$ G. Most MSPs are in binary systems. They are thought to have been spun up by the accretion of matter and thus transfer of angular momentum from a binary companion (Alpar et al. 1992). In some binary systems, the companion is evaporated by the strong relativistic wind produced by the MSP (Ruderman et al. 1989), which becomes isolated, like PSR J0030+0451.

PSR J0030+0451 was discovered by two independent radio surveys, the Arecibo Drift Scan Search (Somer 2000) and the Bologna submillisecond pulsar survey (D'Amico 2000). Its spin-down age τ is 7.6×10^9 yr. The analysis of radio timing residuals showed a significant annual parallax of 3.3 ± 0.9 mas, leading to a distance measurement of 300 ± 90 pc (Lommen et al. 2006), useful for luminosity estimates. The Cordes & Lazio (2002) model of Galactic electron distribution predicts a distance of 317 pc, in good agreement with the parallax measurement. In addition, Lommen et al. (2006) also argued that the Shklovskii effect (Shklovskii 1970) on the pulsar's first period derivative $\dot{P}$ is less than 1%, hence rejecting the possible contamination of proper motion in $\dot{P}$ and reinforcing the determination of the spin-down energy rate $\dot{E}$. This $P = 4.87$ ms and $\dot{P} = 1.0 \times 10^{-20}$ s s^{-1} pulsar hence has an $\dot{E} = 4\pi^2 I(\dot{P}/P^3)$ of 3.5×10^{33} erg s^{-1}, taking the moment of inertia I to be 10^{45} g cm^2. The magnetic field strength at the stellar surface $B_S = 3.2 \times 10^{19}$ G $\sqrt{P\dot{P}}$ for this pulsar is 2.2×10^8 G, and its characteristic age $\tau = P/(2\dot{P})$ is 7.7×10^9 yr.

This pulsar was detected in X-rays with *ROSAT*, during the final days of the mission, shortly after its discovery in radio (Becker et al. 2000). The MSP was then observed by *XMM-Newton* (Becker & Aschenbach 2002). Both telescopes revealed a broad X-ray pulsation profile, with a pulsed fraction compatible with 50% and the two X-ray peaks separated by 0.5 in phase. Unfortunately neither of the two X-ray telescopes could provide the X-ray alignment relative to the radio at the time of the observations, due to the lack of accurate clock calibration. We address this alignment issue below. Becker & Aschenbach (2002) showed that the X-ray spectrum is consistent with being purely thermal. Bogdanov et al. (2008) invoked the presence of a hydrogen atmosphere to model the X-ray spectrum.

Six pulsars were detected in gamma rays with high confidence with the EGRET telescope (Thompson et al. 1999), and more recently AGILE and Large Area Telescope (LAT) reported the detection of pulsed gamma rays from PSR J2021+3651 (Halpern et al. 2008; Abdo et al. 2009b). The LAT also discovered a young pulsar in the supernova remnant CTA1 (Abdo et al. 2008). All eight are normal pulsars. Gamma-ray pulsations with 4.9σ statistical significance were reported for the 2.3 ms pulsar J0218+4232 (Kuiper et al. 2004) with EGRET. No pulsed gamma-ray emission had previously been detected from an MSP (Fierro et al. 1995). LAT observations confirm the detection of gamma-ray emission from PSR J0218+4232 (Abdo et al. (Fermi-LAT Collaboration) 2009c).

The revised EGRET catalog of gamma-ray sources of Casandjian & Grenier (2008) lists the new source EGR J0028+0457 with no 3EG counterpart, with a 95% confidence contour radius of 0.°51. The MSP PSR J0030+0451, for which Harding et al. (2005) predicted a gamma-ray flux superior to that of the marginal EGRET detection PSR J0218+4232, is located 0.°5 from EGR J0028+0457 and was hence suggested as a possible counterpart. The launch of the *Fermi* observatory,

[47] National Research Council Research Associate.

formerly GLAST, on 2008 June 11 provided a new opportunity to study the emission of gamma rays by MSPs.

This paper describes the discovery of pulsations from the isolated pulsar PSR J0030+0451 in the *Fermi* LAT data, making this the first high-confidence detection of a MSP in gamma rays. We also discuss the timing analysis of *XMM-Newton* data with accurate clock calibration, providing the phase alignment of the radio, X-ray and gamma-ray emission relative to each other.

2. OBSERVATIONS AND ANALYSIS

The LAT instrument is described in Atwood et al. (2009). Gamma rays convert to electron–positron pairs in the tracker, consisting of tungsten foils interleaved with layers of silicon microstrip detectors. The tracker provides direction information. Below the tracker is the calorimeter in which particles interact in cesium iodide crystals, giving most of the energy information. The detector is surrounded by the anticoincidence detector, which helps reject the charged cosmic-ray background. The LAT is sensitive to photons with energies below 20 MeV to over 300 GeV. Its large field of view of 2.4 sr, large effective area of 8000 cm^2 on-axis at 1 GeV, improved angular resolution (0.°5 of 68% point-spread function (PSF) containment at 1 GeV for events collected in the "front" section with thin radiator foils), the scanning observing mode, and small trigger dead time of 26.5 μs, make the LAT much more sensitive than EGRET. Ground tests using cosmic-ray muons demonstrated that the LAT measures event times with a precision better than 1 μs. On-orbit satellite telemetry indicates comparable accuracy. The software timing chain from the GPS-based satellite clocks through the barycentering and phase-folding software has been shown to be accurate to better than a few μs (Smith et al. 2008).

PSR J0030+0451 is a very stable pulsar. The timing solution used for this object has been derived from observations made with the Nançay radiotelescope, near Orleans, France. About seven hundred observations starting in 1999 July were used, contemporaneous with the *Fermi* LAT data set and bracketing the *XMM-Newton* observation. Between 1999 and 2002, data were recorded with the Navy Berkeley Pulsar Processor (NBPP) backend. This instrumentation was designed and built at the Naval Research Laboratory in collaboration with the University of California, Berkeley (Backer et al. 1997; Foster et al. 1996). The system covers 1.5 MHz per channel for a total bandwidth of 144 MHz centered at 1360 MHz. In timing mode, the data were folded for 15 minutes over 256 bins covering the full period of the pulsar PSR J0030+0451 (with a resolution of $\simeq$ 20 μs). Since late 2004, times of arrival (TOAs) are obtained from the coherent pulsar instrumentation currently in use at Nançay, the Berkeley–Orléans–Nançay (BON) backend (Theureau et al. 2005; Cognard & Theureau 2006). The coherent dedispersion is performed within 4 MHz channels over a total bandwidth of 64 MHz (128 MHz since July 2008) centered at 1398 MHz. Compared to those recent high-quality data, the old NBPP TOAs were dergaded due to the absence of dedispersion inside the 1.5 MHz channels (also producing large systematics when the pulsar scintillates). The bulk of radio observations were done at 1.4 GHz ((1360 $\pm$ 72 MHz before 2002, 1398 $\pm$ 32 MHz after 2004 and 1398 $\pm$ 64 MHz after 2008). 2 GHz observations were made to better constrain the dispersion measure, necessary for the alignment of pulsar profiles at different wavelengths. The TEMPO[48] package was used to build a timing solution from the recorded radio times of arrival, determined through a standard cross-correlation procedure (Taylor 1992). The mean time of arrival uncertainty is 3.6 μs for the recent BON observations (the bulk of the data), while this is 8.6 μs for all the data set. The post-fit rms is 3.7 μs, fitting for the pulsar's frequency and first derivative, and taking its proper motion into account. The timing parameters used for phase-folding gamma-ray events are given in Table 1, the timing residuals after the fitting procedure are plotted in Figure 1. Doubling the error in the parallax given by TEMPO, and adding in quadrature an additional 0.3 mas uncertainty due to the solar wind, as explained in Lommen et al. (2006), we measure a parallax of 4.1 $\pm$ 0.7 mas, which is consistent with the Lommen et al. value. The dispersion measure we derive is also consistent with the value of 4.3328(3) pc cm^{-3} quoted in Lommen et al. (2006).

The LAT data considered here were taken during *Fermi*'s first-year all-sky survey, starting 2008 August 3, through November 2. The pulsar is located well outside of the Galactic plane (l = 113.°141 and b = −57.°611) and is hence in a region of low Galactic background. Aiming to have a good signal-to-noise ratio over a broad energy range, we used an energy-dependent region of interest of $\theta = \mathrm{Max}[0.9\text{–}2.1\,\mathrm{Log}_{10}(E_{GeV}), 1.5]$ dergees around the pulsar position. A larger fraction of the PSF is included at high energies, where there is little background contamination. Since *Fermi* was operating in survey mode, the contribution of the Earth's gamma-ray albedo to the background was negligible. Finally, the "diffuse" class events were kept. A description of event classes can be found in Atwood et al. (2009).

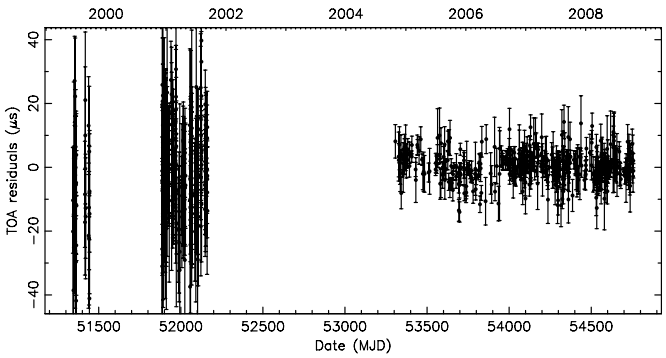

Figure 1. Timing residuals as a function of time for the model given in Table 1. Data between 1999 and 2002 were recorded using the NBPP backend, the BON backend was used after 2004.

Table 1
Timing Ephemeris for Pulsar PSR J0030+0451

Parameter	Value
Right ascension, α	00:30:27.4303(5)
Declination, δ	04:51:39.74(2)
Proper motion in right ascension, μ_α (mas yr^{-1})	−5.3(9)
Proper motion in declination, μ_δ (mas yr^{-1})	−2(2)
Parallax (mas)	4.1(3)
Epoch of position determination (MJD)	52079
Pulse frequency, ν (s^{-1})	205.530699274922(9)
First derivative of pulse frequency, $\dot{\nu}$ (s^{-2})	$-4.2976(4) \times 10^{-16}$
Epoch of ephemeris (MJD)	50984.4
MJD range	51343 – 54757
Number of TOAs	651
Rms timing residual (μs)	3.69
Dispersion measure, DM (cm^{-3} pc)	4.333(1)
Solar system ephemeris model	DE200

Notes. Figures in parentheses are the nominal 1σ TEMPO uncertainties in the least-significant digits quoted. Epochs are given in TDB units.

[48] http://www.atnf.csiro.au.research/pulsar/tempo

After application of the above cuts, we obtained a data set of 563 events over 100 MeV.

PSR J0030+0451 was observed by *XMM-Newton* on 2001 June 19–20. The observations with the pn camera spanned 29 ks, but a soft proton flare affected approximately 8.8 ks of the exposure. The data were reduced using Version 8.0 of the *XMM-Newton* Science Analysis Software.[49] This version solves the timing problem. The pn camera was used in timing mode with the thin filter. The data were reduced using "epproc." The event lists were filtered, so that 0–4 of the predefined patterns (single and double events) were retained, as these have the best energy calibration. We used the data between 0.3 and 2.5 keV as this had the best signal-to-noise ratio. The event times were converted to Barycentric Dynamical Time, using the task "barycen" and the same coordinates as used for the *Fermi* data. The *XMM-Newton* absolute timing accuracy is found to be as good as 300 μs,[50] or $\simeq 0.06$ rotations of PSR J0030+0451. In order to obtain such fine temporal resolution with the pn in timing mode, the CCD is read out continuously, causing the events for the target source to be smeared out in the *Y*-direction. To extract all the events from the source, we used the standard procedure of creating a one dimensional image, by binning all of the raw data in the *Y*-direction into a single bin. The spectrum was extracted using a range of 7 pixels centered on the pulsar, in the *X*-direction. The background spectrum was extracted from a similar neighboring region, free from X-ray sources.

3. RESULTS

3.1. Gamma-Ray and X-ray Profile Analysis

Figure 2 shows the phase histogram of the events with energies greater than 100 MeV in panel a, along with the reference radio profile used to derive the timing ephemeris in panel c. The χ^2 value for the phase histogram shown in panel a of Figure 2 is 121 for 29 dergees of freedom, indicating that the probability that the pulsation is actually a statistical fluctuation is 3.1×10^{-13}. The bin independent *H*-Test (de Jager et al. 1989) gives a value of 123. The derived chance occurrence probability of the null hypothesis, non-pulsed emission, is below 4×10^{-8}. The null hypothesis is hence ruled out, for a single trial.

The zero of phase in the reference radio profile is defined to be at the maximum of the first Fourier harmonic of the signal, transferred back to the time domain. The maximum of the main radio peak's second subpulse is at 0.036 in phase. The gamma-ray pulse profile comprises two peaks (see Figure 2, panel a). There is a shift between the first gamma-ray peak (P1), occurring at 0.15 ± 0.01 in phase, and the main radio peak. The gamma-ray peaks of PSR J0030+0451 are very sharp. We fit P1 and P2 with two-sided Lorentzians, to take into account the different widths for the leading and trailing edges. For the first peak, the fit gives a full width at half-maximum (FWHM) of 0.07 ± 0.01 in phase, that is, 340 μs. The second gamma-ray peak, P2, lags P1 by $\Delta\Phi = 0.44 \pm 0.02$ in phase. The fit of the structure between 0.45 and 0.6 places the peak at 0.59 ± 0.01 in phase with a FWHM of 0.08 ± 0.02 in phase.

LAT phase histograms in two energy bands are given in Figure 3, with 30 bins per rotation. The pulsar is faint in the 100 to 500 MeV band. In this energy band, P2 is prominent relative to P1: taking P1 (resp. P2) between 0.1 and 0.25 in phase (resp. 0.45 and 0.60), the P1/P2 ratio is found to be 0.47 ± 0.17. The upper panel of Figure 3 shows the events with energies over 500 MeV. In this band P1 dominates P2, with a ratio of 1.64 ± 0.48. There, hence, seems to be a spectral dependence of the gamma-ray profile. Within error bars, the P1/P2 ratio seems to increase as a function of energy, conversely to the Vela pulsar (Abdo et al. 2009a). The first gamma-ray peak hence seems harder than the second one. More photons are needed to perform phase-resolved spectroscopy. We note that in the 100 MeV to 500 MeV energy band, P2 seems broader and closer to P1 than it does for energies greater than 500 MeV. However, we cannot be conclusive about this trend due to the low number of photons in P2: more statistics might reveal bridge emission between P1 and P2, in which case P2 would be narrower than the $0.08 + /-0.02$ value quoted above. We also note that there is no evidence for pulsed emission from 20 MeV to 100 MeV. Extrapolation of the hard, observed spectrum (see spectral analysis below) predicts only a few photons in this energy band, and any pulsation is almost certainly obscured by the rapidly rising background below 200 MeV.

The overall gamma-ray emission profile is reminiscent of the younger pulsars Vela, Crab, Geminga, PSR B1951+32, or PSR J2021+3651, especially over 500 MeV. The phase separation of $\simeq 0.4$ between the two peaks is a common feature (Thompson 2004). The pulse profile also shows a main gamma-ray peak lagging the main radio component by 0.15 ± 0.01, similar to the main gamma peak lagging 0.11 to 0.16 after the radio pulse for Vela, PSR B1951+32, and PSR J2021+3651. The

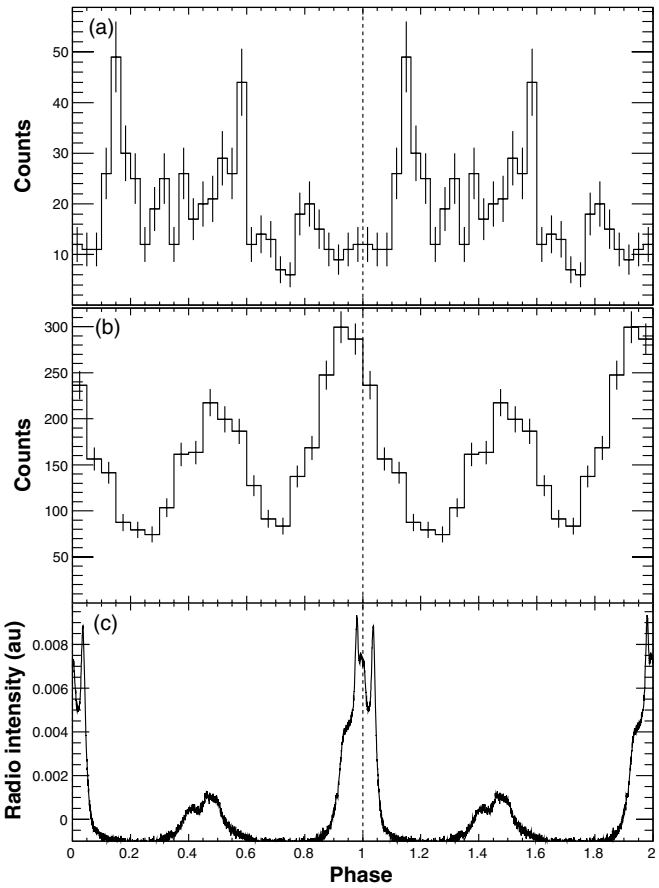

Figure 2. Multi-wavelength phase histograms of PSR J0030+0451. Two pulsar rotations are shown. (a) Gamma-ray phase histogram of PSR J0030+0451 at E > 100 MeV, within an energy-dependent ROI. Each bin is 0.033 in phase, or 160 μs. (b) 20 bin 0.3–2.5 keV *XMM-Newton* phase histogram. (c) Radio profile obtained at 1.4 GHz used to build the ephemeris.

[49] http://xmm.vilspa.esa.es/sas/
[50] http://xmm2.esac.esa.int/docs/documents/CAL-TN-0045-1-0.pdf

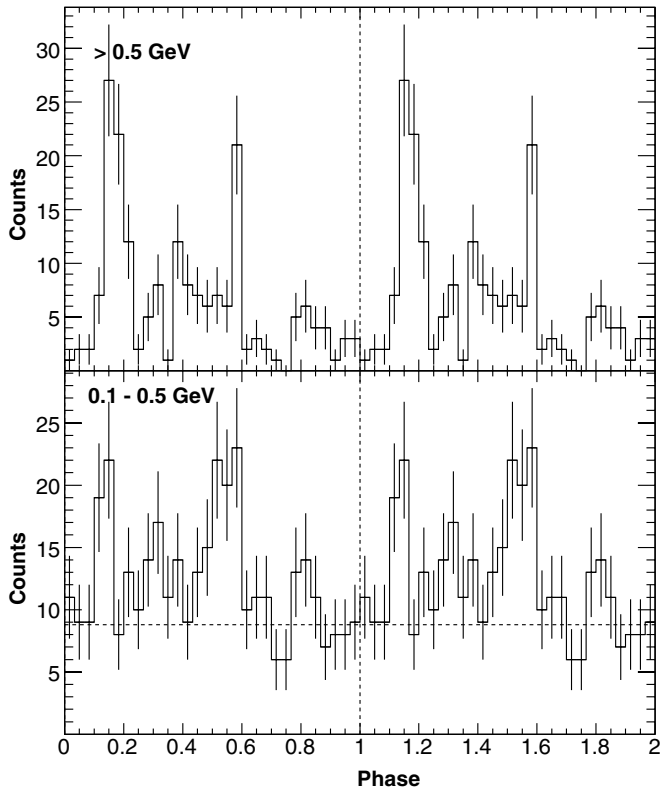

Figure 3. 30 bin phase histograms for PSR J0030+0451 with the LAT, in different energy bands. Two rotations are shown. The horizontal dashed line shows the background level estimated from a surrounding annulus.

radio to P1 and P1 to P2 separations are in agreement with the outer-gap pulse profile model of Romani & Yadigaroglu (1995), which compares the gamma-ray peak separation Δ with the radio to gamma-ray lag δ for a given magnetic inclination angle α. This is also in agreement with the two-pole caustic and slot gap models for gamma-ray emission (Watters et al. 2009; Dyks et al. 2004). With radio polarization measurements, Lommen et al. (2000) found the magnetic inclination angle α to be most probably 62°, that is a mostly orthogonal configuration.

Panel b in Figure 2 shows the 0.3 to 2.5 keV *XMM-Newton* phase histogram for PSR J0030+0451. The overall profile is similar to that found by Becker et al. (2000) and Becker & Aschenbach (2002), though their observations did not yield the X-ray to radio alignment because of inaccurate absolute timing. Here the $\simeq$300 μs absolute timing accuracy represents $\pm$ 1 bin in panel b. The X-ray and radio are hence consistent with being phase aligned. This result supports the idea that the X-ray and radio emission have common origins in the pulsar magnetosphere, and that gamma-rays are produced in a different region. In that sense, PSR J0030+0451 is different from PSR J0218+4232: according to Kuiper et al. (2000), the 2.3 ms pulsar has its radio, X-ray, and gamma-ray components aligned.

3.2. Gamma-ray Spectral Analysis

Using the standard maximum-likelihood spectral estimator *gtlike* in the *Fermi* Science Tools,[51] we performed a spectral analysis of the gamma sample. The diffuse Galactic background and extragalactic emissions are taken into account, as well as the instrument response, which is a function of the photon energy and incidence angle relative to the telescope axis. The data set used for the spectral analysis spans the same time interval as for the timing analysis, but this time we retain events within 15° of the MSP. Because of present uncertainty in the instrument response below 200 MeV, events with energy below 200 MeV are rejected.

[51] http://fermi.gsfc.nasa.gov/ssc/data/analysis/SAE_overview.html

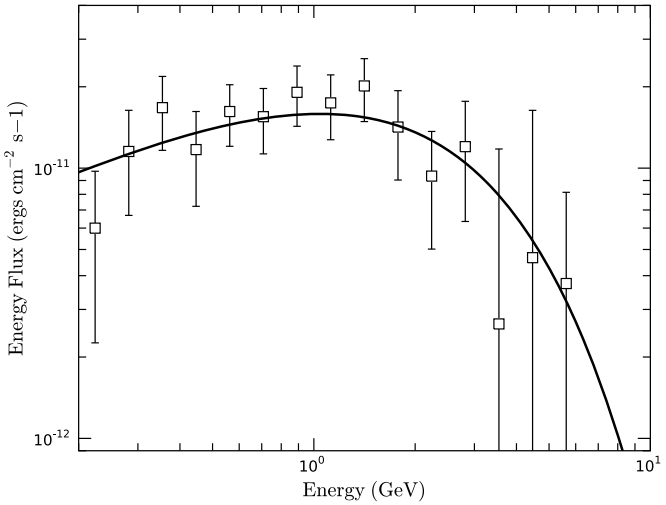

Figure 4. Phase-averaged spectral energy distribution for PSR J0030+0451, along with the best-fit power law with exponential cutoff. Statistical errors are shown.

Figure 4 shows the phase-averaged differential energy spectrum. The corresponding power law with exponential cutoff modeling the data is given by:

$$\frac{dN_\gamma}{dE} = N_0 \left(\frac{E}{10^3\ \mathrm{MeV}}\right)^{-\Gamma} e^{-E/E_c}. \quad (1)$$

In this expression, E is in MeV, the prefactor term $N_0 = (1.84 \pm 0.38 \pm 0.37) \times 10^{-11}$ photons cm^{-2} s^{-1} MeV^{-1}, the power-law index $\Gamma = (1.4 \pm 0.2 \pm 0.2)$, and the cutoff energy $E_c = (1.7 \pm 0.4 \pm 0.5)$ GeV. The first error is statistical, the second is systematic, dominated by differences between the a priori expectations of the *Fermi* LAT effective area and the on-orbit instrument response. The magnitude of this effective area uncertainty is <10% near 1 GeV, 20% below 0.1 GeV, and 30% over 10 GeV. Analysis improvements are underway.

The stability of the results was tested by fitting the same data set with a binned maximum likelihood estimator, "ptlike," which computes the photon counts in a point source weighted aperture in excess of background counts. The fit results, shown in Figure 4 for each energy band, are consistent with those obtained with "gtlike" within error bars. We have also tried a simple power-law fit to the data, of the form $dN_\gamma/dE = N_0(E/1\ \mathrm{GeV})^{-\Gamma}$. The fit using the exponential cutoff functional form is better constrained, with a difference in the log likelihoods of 10.76. A χ^2 interpretation of this value leads to a probability of incorrectly rejecting the power-law hypothesis of 3.5×10^{-6}.

Intergating Equation (1) for energies >100 MeV yields an integral flux $f_{>100\ \mathrm{MeV}} = (6.76 \pm 1.05 \pm 1.35) \times 10^{-8}$ photons cm^{-2} s^{-1}. The revised EGRET catalog of Casandjian & Grenier (2008) quotes a flux of $(10.4 \pm 3.1) \times 10^{-8}$ photons cm^{-2} s^{-1} for EGR J0028+0457, based on the summed EGRET data set. Both fluxes are statistically in agreement. The pulsar is in a low EGRET exposure region, mainly detected at large off-axis angles where systematic uncertainties in the effective area were large.

The energy flux is $F_{\rm obs} = (4.91 \pm 0.45 \pm 0.98) \times 10^{-11}$ erg cm^{-2} s^{-1} over 100 MeV. The luminosity of a pulsar can be written as $L_\gamma = 4\pi f_\Omega F_{\rm obs} D^2$, where D is the pulsar distance, f_Ω is a correction factor containing information about the beaming geometry, and $F_{\rm obs}$ is the observed phase-averaged energy flux. Watters et al. (2009) have computed pulse profiles and f_Ω corrections for young pulsars. The outer magnetospheres for MSPs should be scaled-down analogues of those of young pulsars. If we use the maps in Watters et al. (2009) for a pulse separation $\Delta = 0.4$ and a magnetic inclination $\alpha = 62^\circ$, as inferred from the radio polarization data, we find a reasonable match for an old, high-efficiency two-pole caustic/slot gap model for a viewing angle $\zeta \simeq 75^\circ$. In turn this implies $f_\Omega \simeq 0.8$. This pulse width is not natural in a high efficiency, large gap width outer gap model, suggesting that the lower altitude two-pole caustic picture is a better match to the data, unless the true pulsar efficiency is $\lesssim 0.1$. Adopting $f_\Omega = 1$ for PSR J0030+0451, we obtain an efficiency $\eta = L_\gamma/\dot{E} = 15\%$ for the conversion of spin-down energy into gamma-ray emission.

Arons (1996) noted that for the EGRET pulsars, η is, in good approximation, inversely proportional to the open field line voltage $V = 4 \times 10^{20} P^{-3/2} \dot{P}^{1/2}$, proportional to $\sqrt{\dot{E}}$, and also proportional to the open field current (Harding 1981). With an open field line voltage of 1.2×10^{14} volts and an efficiency of 15%, PSR J0030+0451 seems to break from the trend, which would predict a higher value. However, the efficiency law may saturate at lower spin-down rates. Other low $\dot{E}$ pulsar detections with *Fermi* should help constrain how these old "recycled" pulsars convert their energy-loss rate into gamma-ray luminosity. In addition, the discovery of pulsed emission from PSR J0030+0451, which has a smaller spin-down rate than previously known gamma-ray pulsars, lowers the empirical $\dot{E}$ threshold for gamma-ray emission by an order of magnitude. This suggests that many low $\dot{E}$ pulsars might be detectable by the LAT.

Attempts to describe the high-energy emission from MSPs were recently made based on the two main classes of theoretical models: the polar cap (PC) and the outer gap (OG) models. In the PC description by Harding et al. (2005), charged particles are accelerated along the open field lines near the magnetic poles to high altitudes. The high-energy spectrum consists of three main components. The emission of photons up to 100 MeV is dominated by synchrotron radiation from electrons. Over 100 GeV, photons are produced by inverse Compton radiation from electrons. Curvature radiation from electrons dominates the photon spectrum between 1 and 100 GeV. For PSR J0030+0451, Harding et al. (2005) provide a prediction of 4.25 GeV for the curvature radiation cutoff energy. This value differs from the 1.7 GeV we find in this analysis. In their model, the expected curvature radiation flux over 100 MeV is $F_{\rm CR}(> 100\ {\rm MeV}) \sim 3 \times 10^{-6}$photons cm^{-2} s^{-1} for our pulsar. Our measured intgral flux disagrees with their expectation. However, Harding et al. (2005) computed sky-averaged spectra; more detailed three-dimensional sums may be needed to make predictions for an individual viewing angle. On the other hand, in the OG description of the high-energy radiation from MSPs by Zhang & Cheng (2003), a strong multipole magnetic field exists near the stellar surface. X-rays are then produced by the backflow current of the outer gap, which is a vacuum gap close to the light cylinder. These X-rays consist of a non-thermal power-law component, plus two thermal components. Gamma-rays are produced in the outer gap. Though Zhang & Cheng (2003) provide no application of their model to the case of PSR J0030+0451, they predict that a gamma-ray MSP would be an X-ray MSP. This is indeed the case for both PSR J0030+0451 and PSR J0218+4232. Secondly, they predict that if the X-ray spectrum is dominated by thermal emission, which is indeed the case for PSR J0030+0451, consistent with being purely thermal (Becker & Aschenbach 2002), the gamma-ray emission can extend to ~GeV gamma-rays only, as we observe.

4. CONCLUSION

We described the detection of the MSP PSR J0030+0451 in gamma-rays using the *Fermi* LAT. We now have high confidence that there are gamma-ray emitters among MSPs. This provides a new tool for studying the magnetospheres of energetic pulsars. Detection of more MSPs in the LAT data may invite revisiting the possible contribution of unresolved MSPs to the overall Galactic diffuse emission in the gamma-ray band: for instance Wang et al. (2005) proposed that the Galactic center might contain a few thousand unresolved MSPs, contributing to the diffuse spectrum detected by EGRET, which shows a break at a few GeV. One might also expect cumulative gamma-ray emission of MSPs in globular clusters, such as 47 Tuc, which is thought to contain up to 60 MSPs (Camilo & Rasio 2005). The EGRET search for emission from globular clusters only provided upper limits (Michelson et al. 1994; Fierro et al. 1995). The *Fermi* LAT offers new opportunities to search for emission from globular clusters in gamma rays.

The *Fermi* LAT Collaboration acknowledges generous ongoing support from a number of agencies and institutes that have supported both the development and the operation of the LAT as well as scientific data analysis. These include the National Aeronautics and Space Administration and the Department of Energy in the United States, the Commissariat à l'Energie Atomique and the Centre National de la Recherche Scientifique/Institut National de Physique Nucléaire et de Physique des Particules in France, the Agenzia Spaziale Italiana and the Istituto Nazionale di Fisica Nucleare in Italy, the Ministry of Education, Culture, Sports, Science and Technology (MEXT), High Energy Accelerator Research Organization (KEK) and Japan Aerospace Exploration Agency (JAXA) in Japan, and the K. A. Wallenberg Foundation, the Swedish Research Council and the Swedish National Space Board in Sweden.

Additional support for science analysis during the operations phase from the following agencies is also gratefully acknowledged: the Istituto Nazionale di Astrofisica in Italy and the K. A. Wallenberg Foundation in Sweden for providing a grant in support of a Royal Swedish Academy of Sciences Research fellowship for J.C.

REFERENCES

Abdo, A. A. et al. (Fermi-LAT Collaboration) 2008, Science, 322, 1218
Abdo, A. A., et al. (Fermi-LAT Collaboration) 2009a, ApJ, 696, 1084
Abdo, A. A., et al. (Fermi-LAT Collaboration) 2009b, ApJ, submitted
Abdo, A. A., et al. (Fermi-LAT Collaboration) 2009c, Science, submitted
Alpar, M. A., et al. 1992, Nature, 300, 728
Arons, J. 1996, A&AS, 120, 49
Atwood, W. B., et al. (Fermi-LAT Collaboration) 2009, ApJ, in press
Becker, W., & Aschenbach, B. 2002, in Proc. 270, WE-Heraeus Seminar on Neutron Stars, Pulsars, and Supernova Remnants, ed. W. Becker, H. Lesch, & J. Trümper (MPE Report 278; Garching: MPI), 64
Becker, W., Trûmper, J., Lommen, A.N., & Backer, D. C. 2000, ApJ, 545, 1015
Backer, D. C., et al. 1997, PASP, 109, 61
Bogdanov, S., Grindlay, J. E., & Rybicki, G. B. 2008, ApJ, 689, 407

Camilo, F., & Rasio, F. A. 2005, in ASP Conf. Ser., 328, Binary Radio Pulsars, ed. F. Rasio & I. Stairs (San Francisco, CA: ASP), 147
Casandjian, J. M., & Grenier, I. A. 2008, A&A, 489, 849
Cognard, I., & Theureau, G. 2006, in IAU Symp 26, On the Present and Future of Pulsar Astronomy (Cambridge: Cambridge Univ. Press), 36
Cordes, J. M., & Lazio, T. J. 2002, arXiv:astro-ph/0207156
D'Amico, N. 2000, in ASP Conf. Ser. 202, Pulsar Astronomy—2000 and Beyond, ed. M. Kramer, N. Wex, & N. Wielebinski (San Francisco, CA: ASP), 27
de Jager, O. C., Swanepoel, J. W. H., & Raubenheimer, B. C. 1989, A&A, 221, 180
Dyks, J., Harding, A. K., & Rudak, B. 2004, ApJ, 606, 1125
Fierro, J. M., et al. 1995, ApJ, 447, 807
Foster, R. S., et al. 1996, in ASP Conf. Ser. 105, Pulsars: Problems and Progress, ed. S. Johnston, M. A. Walker, & M. Bailes (San Francisco, CA: ASP), 25
Halpern, J. P., et al. 2008, ApJ, 688, 33
Harding, A. K. 1981, ApJ, 245, 267
Harding, A. K., Usov, V. V., & Muslimov, A. G. 2005, ApJ, 622, 531
Kuiper, L., Hermsen, W., & Stappers, B. 2004, Adv. Space. Res., 33, 507
Kuiper, L., et al. 2000, A&A, 359, 615
Lommen, A. N., et al. 2000, ApJ, 545, 1007
Lommen, A. N., et al. 2006, ApJ, 642, 1012
Manchester, R. N., Hobbs, G. B., Teoh, A., & Hobbs, M. 2005, AJ, 129, 1993
Michelson, P. F., et al. 1994, ApJ, 435, 218
Romani, R. W., & Yadigaroglu, I. A. 1995, ApJ, 438, 314
Ruderman, M., Shaham, J., & Tavani, M. 1989, ApJ, 336, 507
Shklovskii, I. S. 1970, Sov. Astron., 13, 562
Smith, D. A., et al. 2008, A&A, 492, 923
Somer, A. 2000, in ASP Conf. Ser. 202, Pulsar Astronomy—2000 and Beyond, ed. M. Kramer, N. Wex, & N. Wielebinski (San Francisco, CA: ASP), 17
Taylor, J. H. 1992, Phil. Trans. Roy. Soc. A, 341, 117
Theureau, G., et al. 2005, A&A, 430, 373
Thompson, D. J., et al. 1999, ApJ, 516, 297
Thompson, D. J. 2004, in Cosmic Gamma-Ray Sources, Vol. 304, Gamma Ray Pulsars, ed. K. S. Cheng (Dordrecht: Kluwer), 149
Wang, W., Jiang, Z. J., & Cheng, K. S. 2005, MNRAS, 358, 263
Watters, K. P., Romani, R. W., Weltevrede, P., & Johnston, S. 2009, ApJ, 695, 1289
Zhang, L., & Cheng, K. S. 2003, A&A, 398, 639